

give a width of 1.5 keV ($\frac{1}{4}$ point - $\frac{3}{4}$ point), which probably represents the width of the resonance. However, since instrumental broadening of this amount cannot be ruled out in these data, this value is considered an upper limit, $\Gamma_{\text{tot}} < 1.5$ keV, which leads to a reduced width, $\gamma^2 < 0.13 \times 10^{-13}$ MeV-cm, less than 0.01 times the Wigner limit $3\hbar^2/2\mu a$. This small value may be compared with the reduced particle width of 0.50 times the Wigner limit for the "good" $d_{5/2}$ level at 5.10 MeV.⁹

In summary, the state in F^{17} at 3.86 MeV has $J^\pi = \frac{5}{2}^-$ and very small radiation and particle widths, and so does not exhibit a strong single-particle character. This is satisfying since an "inverted" $f_{5/2,7/2}$ structure would be very disturbing. The long-standing difficulty of explaining an $f_{7/2}$ level within 4 MeV of the $d_{5/2}$ ground state and below the $d_{3/2}$ level has been removed. The lowest $f_{7/2}$ level now appears to lie^{9,10} at 5.7 MeV, with $\gamma^2/(3\hbar^2/2\mu a) \approx 0.1$ and 0.04 in O^{17} and F^{17} , respectively. The situation for the $\frac{5}{2}^-$ level in O^{17} is less clear. Since it is bound, it is necessary to appeal to widths obtained in (d, p) stripping. At $E_d = 15$ MeV, Keller¹¹ observes a very good stripping pattern and a reduced width which, though small, is perhaps a quarter of that expected³ for a good f level. Nevertheless, the relative reduced width is probably significantly less than for the $\frac{7}{2}^-$ level at 5.7 MeV.^{10,11}

We are indebted to M. H. Macfarlane for several provocative discussions.

*Work performed under the auspices of the U. S. Atomic Energy Commission.

¹C. Broude, T. K. Alexander, and A. E. Litherland, *Bull. Am. Phys. Soc.* **8**, 26 (1963).

²F. Ajzenberg-Selove and T. Lauritsen, *Nucl. Phys.* **11**, 1 (1959).

³M. H. Macfarlane and J. B. French, *Rev. Modern Phys.* **32**, 567 (1960).

⁴R. A. Laubenstein and M. J. W. Laubenstein, *Phys. Rev.* **84**, 18 (1951).

⁵R. W. Harris, G. C. Phillips, and C. M. Jones, *Nucl. Phys.* **38**, 259 (1962).

⁶The targets were prepared by the technique of J. Bair and H. Willard, *Bull. Am. Phys. Soc.* **6**, 440 (1961), as modified by J. A. Weinman, Argonne National Laboratory Report ANL-6603, 1962 (unpublished), p. 47.

⁷We use the value 3.470 MeV as the resonant bombarding energy. Relative to this value, the bombarding energies are good to about 1 keV.

⁸D. H. Wilkinson, *Nuclear Spectroscopy*, edited by F. Ajzenberg-Selove (Academic Press, Inc., New York, 1960), Part B, p. 852.

⁹S. R. Salisbury and H. T. Richards, *Phys. Rev.* **126**, 2147 (1962). For the sake of uniformity, the reduced widths given here conform with those quoted by these authors. It should be emphasized that the ratio for the two states (50:1) is practically independent of the mode of calculation (e.g., the radius used).

¹⁰R. O. Lane and J. E. Monahan, *Bull. Am. Phys. Soc.* **3**, 364 (1958); Argonne National Laboratory Report ANL-5937, November, 1958 (unpublished), p. 4. The radius used in calculating the neutron width 0.1 gives a width of 0.5 for the $d_{3/2}$ level.

¹¹E. L. Keller, *Phys. Rev.* **121**, 820 (1961).

BETA-DECAY ASYMMETRY AND NUCLEAR MAGNETIC MOMENT OF NEON-19[†]

Eugene D. Commins* and David A. Dobson

Department of Physics, University of California, Berkeley, California

(Received 18 March 1963)

The angular distribution of decay electrons from polarized beta-radioactive spin- $\frac{1}{2}$ nuclei is given by¹

$$I(\theta) = 1 + A(v/c) \cos\theta \quad (1)$$

where v is the electron velocity, c is the velocity of light, and θ is the angle between the electron velocity vector and the spin polarization axis. We have determined the asymmetry parameter A of neon-19, and have measured the nuclear magnetic moment of neon-19 by observing the reversal of beta-decay asymmetry which occurs when polarized neon-19 nuclei undergo resonance

reorientation. The results are

$$A(\text{Ne}^{19}) = -0.057 \pm 0.005$$

$$\mu(\text{Ne}^{19}) = -1.886 \pm 0.001 \text{ nm.}$$

In both of these results we assume $I = \frac{1}{2}$ and $\mu < 0$.² The result for A leads to an interesting interpretation of the relative sign of Fermi and Gamow-Teller matrix elements in Ne^{19} decay. The result for μ provides a useful datum in the study of the structure of light nuclei.

The experimental method is as follows: A beam of neon-19 in the 1S_0 ground state emerges from an atomic beam source at 77°K and trav-

erases an inhomogeneous magnetic deflecting field ("A" field) of the conventional type.³ The beam is thereby split into two spatially separated "half" beams, corresponding to $m_I = \pm \frac{1}{2}$. The "A" magnet is 44 cm long and provides a field gradient up to 50 kG/cm. A movable collimating slit 0.015 cm wide is located halfway along the "A" magnet. The beam emerges from the "A" magnet, passes through an rf transition region in a homogeneous "C" field ($H_C \cong 1140$ gauss), where nuclear resonance reorientation may be induced, and proceeds through a Pyrex channel of length 3.80 cm. The width and height of the channel are 0.038 cm and 0.475 cm, respectively. The entrance to the channel is effectively the detector aperture for the beam. By moving the collimator in the "A" magnet, different portions of the beam are allowed to strike the detector aperture. If the collimator is more than 0.012 cm to one side of center a portion of only one "half" beam can enter the channel and the nuclei in this beam are completely polarized in one direction. By moving the collimator the same amount to the other side of center, the polarization is reversed. When the collimator is in the center equal amounts of both "half" beams are transmitted through the channel and the net polarization is zero. The polarization can also be (partially) reversed for a given "half" beam by nuclear resonance reorientation in the "C"-field region.

The channel terminates in a cylindrical Pyrex bulb 6.6 cm long and 4 cm in diameter, with slightly concave end walls about 0.010 cm thick. The bulb is situated in a homogeneous magnetic field H_D (usually about 230 gauss) which is parallel to H_C , H_A , and the bulb axis. (See Fig. 1.) The walls of the bulb and channel are coated with a thin layer of Teflon to inhibit nuclear spin relaxation which might occur on wall collisions.⁴

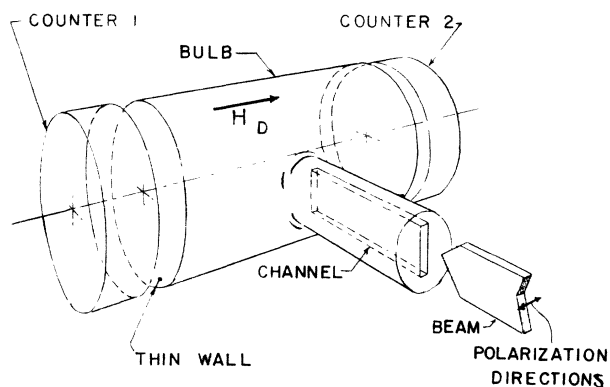


FIG. 1. View of detector bulb and Geiger counters (not to scale).

The atoms entering the bulb remain there for a mean time $\tau = V/S \cong 12$ seconds, where $V = 80$ cm³ is the volume of the bulb, and $S = 6.5$ cm³/sec is the conductance of the channel. Since the half-life of neon-19 is 18.5 seconds, approximately 35% of the atoms entering the bulb decay there. Those positrons which are emitted in the directions of the end walls penetrate them with relatively small energy loss and are detected by two thin-windowed Geiger counters, one adjacent to each end wall. The orbits of the positrons (average energy 1 MeV, maximum energy 2.235 MeV) are not appreciably affected by H_D . In spite of the long time τ , during which the average atom makes 10^5 wall collisions, relaxation of nuclear spin polarization is negligible ($T_1 \gg \tau$) and the positron emission is asymmetric.

For a given collimator position corresponding to a definite state of nuclear polarization in the bulb, counts N_1 and N_2 are obtained during three-minute time intervals from counters 1 and 2. After a small background correction is made, $(N_1 + N_2)$ is proportional to beam intensity. In Fig. 2, beam intensity is plotted versus col-

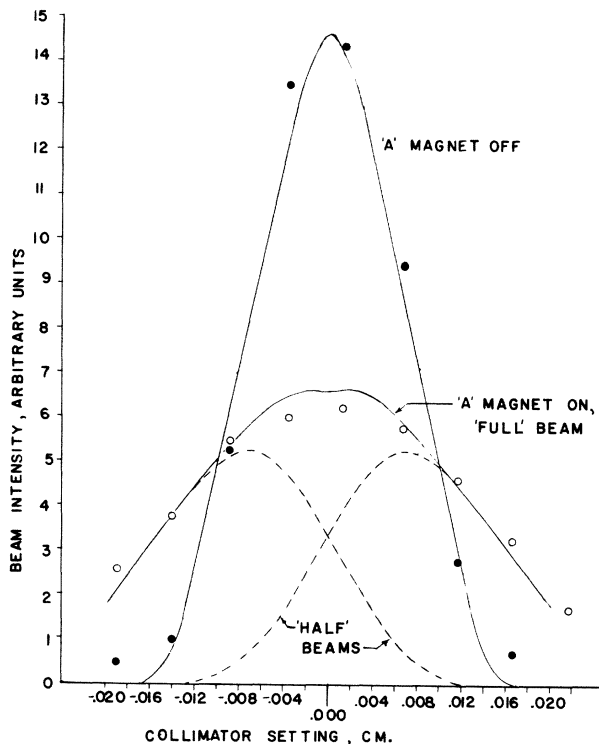


FIG. 2. Beam intensity versus collimator position. The full curves are calculated intensity patterns. The dashed curves represent the contribution of each "half" beam to the intensity obtained with magnet on. The circles are experimental points; black corresponds to magnet off and white to magnet on.

limator setting, for "A" magnet on and off. The curves in Fig. 2 show the calculated intensity patterns⁵ from each half-beam and their sum, assuming $\mu = -1.9$ nm and $\nabla H = 4.5 \times 10^4$ G/cm. The calculated magnet-off pattern is also shown. It can be seen from Fig. 2 that collimator settings >0.012 cm on either side of center correspond to complete polarization.

The asymmetry is determined from the quantity $R = (N_1 - N_2)/(N_1 + N_2)$. R is not in itself significant because it depends, among other things, on background level, differences in counter efficiencies and bulb end-wall thicknesses, etc. However, by changing the collimator setting and thus the nuclear polarization we change R . After applying a background correction obtained by setting the collimator far from center so that no beam enters the channel, the quantity $\Delta = R_+ - R_-$ is directly proportional to the asymmetry parameter A . R_+ corresponds to complete positive polarization, $m_I = +\frac{1}{2}$, and R_- corresponds to $m_I = -\frac{1}{2}$. Taking into account the geometry of the bulb and counters, the positron energy distribution,⁶ and the effects of energy loss in the bulb end walls and counter windows, calculation shows that $A = 1.20 \Delta$ for the 80-cm³ bulb.

The quantity Δ was determined on many separate occasions with bulbs ranging in volume from 30 cm³ to 80 cm³, and with various channel lengths and wall coatings (Teflon, Parafint, heated bare Pyrex). The range in τ was from 2 to 12 seconds. Three Teflon-coated bulbs were used, and for each of these the asymmetry was stable and reproducible. For the other bulbs the asymmetry was not stable, presumably because T_1 was comparable to τ and variable in time. We never observed any asymmetry with these bulbs which was larger than that observed with the Teflon-coated bulbs.

The final value of A was obtained from 114 separate pairs of 3-minute observations of Δ in the 80-cm³ Teflon-coated bulb described in detail above. The nuclear moment μ was determined by observing a change in the sign of Δ accompanying resonance reorientation. The rf field in the transition region was generated by a hairpin 0.8 cm long excited by a power amplifier driven by a Tektronix Type 190A signal generator. The input frequency was monitored with a Hewlett-Packard Model 524C frequency counter. H_C was determined by inserting a proton resonance probe in the transition region at various times during the run. The permanent "C" field H_C varied by less than one part in 1000 during the

course of the experiment. Small fluctuations were caused mainly by drifts in the fringing field of the "A" magnet. A partial reversal of asymmetry was also observed when the field H_D was reversed, if a small external field at right angles to H_C and H_D was applied between them. If this field was not applied, Majorana transitions were observed when H_D was reversed, presumably because the beam passed through a region of "zero" field. Figure 3 shows Δ as a function of applied frequency in the neighborhood of resonance. The center of the line may be determined by inspection to within about 1 kc/sec. The observed linewidth and required rf power are consistent with the length of the hairpin and the beam velocity.

Neon-19 is produced using the reaction $F^{19}(p, n)Ne^{19}$ by bombardment of a target containing SF_6 gas at 2.5 atmospheres pressure, with a 13-MeV proton beam from the Livermore 90-in. cyclotron. The SF_6 gas flows continuously through the target chamber and carries neon-19 with it from the target to the experimental site through about 60 feet of $\frac{1}{4}$ -inch copper tubing. The SF_6 is condensed in a liquid N_2 trap near the apparatus and neon-19 flows on to the atomic beam source. Preliminary experiments were done at the Berkeley 60-in. cyclotron prior to its demolition in June, 1962.

The asymmetry parameter $A(Ne^{19})$ is given by the following theoretical expression⁷:

$$A(Ne^{19}) = \frac{(2/3)|C_A|^2|\langle\sigma\rangle|^2 + (2/\sqrt{3})|C_A||C_V|\langle 1|\langle\sigma\rangle}{|C_V|^2|\langle 1\rangle|^2 + |C_A|^2|\langle\sigma\rangle|^2}$$

where C_V and C_A are the vector and axial vector coupling constants respectively, and $\langle 1\rangle$ and $\langle\sigma\rangle$ are the Fermi and Gamow-Teller matrix elements, respectively. The first term on the right-hand side is positive, so that $A = -0.057$ implies $\langle 1|\langle\sigma\rangle < 0$ and $|C_A\langle\sigma\rangle/C_V\langle 1\rangle|^2 = 2.38$. For the purpose of a qualitative argument it is assumed that the ground-state configuration of the Ne^{19} nucleus is $s_{1/2}^2(p)s_{1/2}(n)$. It may then seem surprising that $\langle 1|\langle\sigma\rangle$ is negative in Ne^{19} decay but positive in the decay of the neutron.⁸ However, in N^{19} the configuration $s_{1/2}^2(p)s_{1/2}(n)$ is equivalent to a "hole" in the configuration $s_{1/2}^2(p)s_{1/2}^2(n)$, and decay of the "hole" and decay of a single $s_{1/2}$ neutron yield opposite signs for the interference term $\langle 1|\langle\sigma\rangle$. The proof assumes charge independence of nuclear forces. Let

$$\chi^a = (2)^{-1/2}(\alpha_1\beta_2 - \beta_2\alpha_1)\alpha_3$$

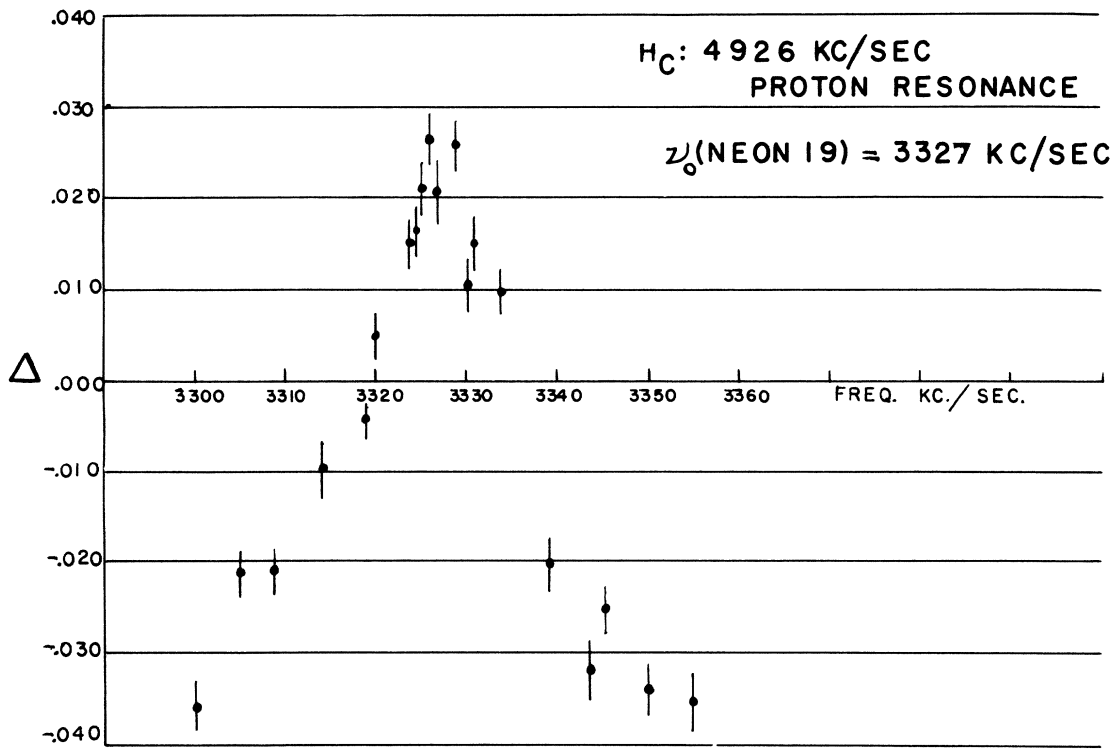


FIG. 3. Reversal of beta-decay asymmetry in the neighborhood of resonance. The error flags on the experimental points are computed statistical probable errors.

and

$$\chi^S = (6)^{-1/2}[(\alpha_1\beta_2 + \beta_2\alpha_1)\alpha_3 - 2\alpha_1\alpha_2\beta_3]$$

be antisymmetric and symmetric $I = \frac{1}{2}$ spin functions respectively, made up from three nucleons of spin $\frac{1}{2}$. As usual α refers to spin up, β to spin down. For $T = \frac{1}{2}$, antisymmetric and symmetric isotopic spin functions are similar to the foregoing:

$$\xi^a = (2)^{-1/2}(pn - np)p$$

and

$$\xi^S = (6)^{-1/2}[(pn + np)p - 2ppn].$$

Here p and n stand for $\tau_3 = \pm 1$ eigenfunctions respectively. The fully antisymmetrized neon-19 state is

$$|\text{Ne}^{19}\rangle = (2)^{-1/2}(\chi^a \xi^S - \chi^S \xi^a). \quad (2)$$

We generate the F^{19} state ($T_3 = -\frac{1}{2}$) by applying the operator $T_- = T_1 - iT_2$ to the Ne^{19} state:

$$|F^{19}\rangle = T_- |\text{Ne}^{19}\rangle.$$

The Fermi matrix element is

$$\langle 1 | = \left\langle \sum_{i=1}^3 \tau_-^i \right\rangle = \langle F^{19} | T_- | \text{Ne}^{19} \rangle = +1.$$

The Gamow-Teller matrix element is

$$\begin{aligned} \langle \sigma \rangle &= \sqrt{3} \left\langle F^{19} \left| \sum_{i=1}^3 \sigma_3^i \tau_-^i \right| \text{Ne}^{19} \right\rangle \\ &= \sqrt{3} \left\langle \text{Ne}^{19} \left| \sum_{ij} \tau_+^j \sigma_3^i \tau_-^i \right| \text{Ne}^{19} \right\rangle. \end{aligned}$$

Since $[\tau_+^j, \tau_-^i] = \delta_{ij} \tau_3^i$ we find from Eq. (2)

$$\langle \sigma \rangle = \sqrt{3} \left\langle \text{Ne}^{19} \left| \sum_{i=1}^3 \sigma_3^i \tau_3^i \right| \text{Ne}^{19} \right\rangle = -\sqrt{3}.$$

In fact the Ne^{19} ground-state configuration is probably not simply^{9,10} $s_{1/2}^2(p)s_{1/2}(n)$ but this evidently does not alter the main conclusion, which is that $\langle \sigma \rangle < 0$. The result $|C_A \langle \sigma \rangle / C_V \langle 1 \rangle|^2 = 2.38$ is consistent with the experimentally determined ft value of Ne^{19} , which yields $|C_A \langle \sigma \rangle / C_V \langle 1 \rangle|^2 = 2.43 \pm 0.13$ assuming $\langle 1 \rangle = 1$ and the value of C_V determined from decay of O^{14} .¹¹

We gratefully acknowledge an illuminating correspondence with Professor E. J. Konopinski of Indiana University, who made clear to us the

role of isotopic spin in calculation of the sign of A . Thanks are due the staffs of the 60-in. and 90-in. cyclotrons for their unfailing cooperation, and Professor E. Wichmann of the University of California for several helpful discussions.

†Work supported jointly by the U. S. Atomic Energy Commission and the National Science Foundation.

*Alfred P. Sloan Foundation Fellow.

¹E. J. Konopinski, *Ann. Rev. Nucl. Sci.* **9**, 104 (1959).

²D. Strominger, John M. Hollander, and Glenn T. Seaborg, *Rev. Mod. Phys.* **30**, 608 (1958).

³N. F. Ramsey, *Molecular Beams* (Clarendon Press, Oxford, 1956), p. 399.

⁴The use of Teflon was suggested by N. F. Ramsey in private conversation.

⁵Ref. 3, p. 349, especially equation XIII.11.

⁶E. Fermi, *Elementary Particles* (Yale University Press, New Haven, 1951), p. 42.

⁷Ref. 1, p. 131, equations 65, 68, 69.

⁸Ref. 1, pp. 116-124.

⁹M. G. Redlich, *Phys. Rev.* **99**, 1421, 1427 (1955).

¹⁰J. P. Elliott and A. M. Lane, *Handbuch der Physik* (Springer Verlag, Berlin, 1957), Vol. 39, p. 350.

¹¹W. P. Alford and D. R. Hamilton (Ne^{18} f value), *Phys. Rev.* **105**, 673 (1957).

TECHNIQUE FOR ELIMINATING INTERFERENCE EFFECTS AND BIASES FROM OVERLAPPING RESONANCES

Philippe Eberhard and Morris Pripstein

Laboratoire de Physique Atomique et Moléculaire, Collège de France, Paris, France

(Received 6 March 1963)

We consider the case of a reaction with three particles (1, 2, 3) in the final state where two resonances A and B occur, one in the system of particles 1, 2 and the other in the system of particles 2, 3, and with invariant masses which cross on the Dalitz plot [Fig. 1(a)] for the reaction. The events on the Dalitz plot fall into any one of the four categories listed in Table I. For each

event which occurs in the overlap region AB , no distinction can be made as to which process it represents (α , β , γ or δ). As a result, physicists have either (a) ignored the events in region AB or (b) considered the events in region AB to be all of one type α (or β) when studying the production and decay properties of resonance A (or B).

We have considered the biases introduced by both (a) and (b) and found a technique to eliminate them – a technique which has not yet been described in the literature, to the best of our knowledge. We illustrate the method by applying it to a study of the properties of resonance B in process β .

We introduce and define the following quantities; \hat{p}_2 , \hat{p}_3 , \hat{p}_B , \hat{p}_i are unit vectors in the directions

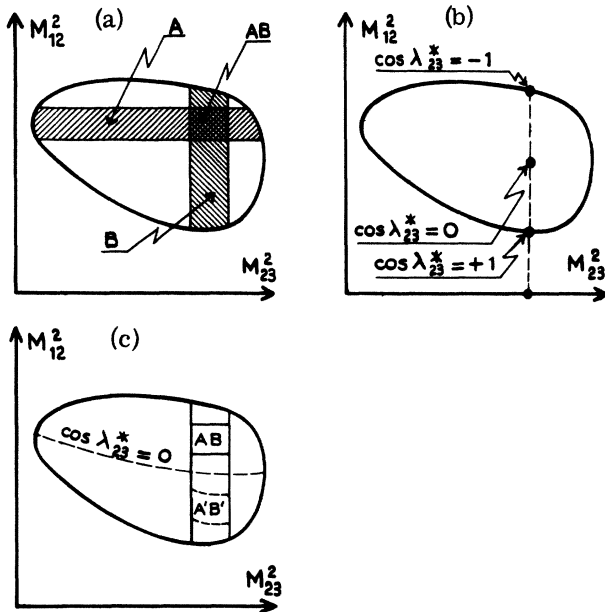


FIG. 1. Typical Dalitz plot (a) showing resonance bands A and B , (b) showing relationship between M_{12}^2 and $\cos \lambda_{23}^*$, (c) showing overlap region AB and its conjugate $A'B'$. Dashed line indicates line for $\cos \lambda_{23}^* = 0$.

Table I. Possible configuration of particles 1, 2, 3 in final state.

Process	Configuration in final state	Position on Dalitz plot for event of this type
α	$A+3$ ↳ $1+2$	In band A
β	$B+1$ ↳ $2+3$	In band B
γ	Interference between processes α and β	In the overlap region AB of bands A and B
δ	$1+2+3$ Nonresonating	Anywhere within the ellipse